JACC: CARDIOVASCULAR IMAGING
VOL. 10, NO. 4, 2017

ISSN 1936-878X/$36.00
PUBLISHED BY ELSEVIER
http://dx.doi.org/10.1016/j.jcmg.2016.05.019

FFR Derived From Coronary CT Angiography in Nonculprit Lesions of Patients With Recent STEMI

Sara Gaur, MD, PhD,[a] Charles A. Taylor, PhD,[b,c] Jesper M. Jensen, MD, PhD,[a] Hans Erik Bøtker, MD, PhD, DMSc,[a] Evald H. Christiansen, MD, PhD,[a] Anne K. Kaltoft, MD, PhD,[a] Niels R. Holm, MD,[a] Jonathon Leipsic, MD,[d] Christopher K. Zarins, MD,[b,e] Stephan Achenbach, MD, PhD,[f] Sophie Khem, MS,[b] Alan Wilk, BS,[b] Hiram G. Bezerra, MD, PhD,[g] Jens F. Lassen, MD, PhD,[a] Bjarne L. Nørgaard, MD, PhD[a]

ABSTRACT

OBJECTIVES This study sought to determine the diagnostic performance of noninvasive fractional flow reserve (FFR) derived from coronary computed tomography angiography (CTA) (FFR_{CT}) for the diagnosis of lesion-specific ischemia in nonculprit vessels of patients with recent in ST-segment elevation myocardial infarction (STEMI).

BACKGROUND In patients with stable angina, FFR_{CT} has high diagnostic performance in identification of ischemia-causing lesions. The potential value of FFR_{CT} for assessment of multivessel disease in patients with recent STEMI has not been evaluated.

METHODS Coronary CTA with calculation of FFR_{CT} and invasive coronary angiography with FFR were performed 1 month after STEMI in patients with multivessel disease. Coronary CTA and invasive coronary angiography stenosis >50% were considered obstructive. Lesion-specific ischemia was assumed if FFR_{CT} was ≤0.80. FFR ≤0.80 was the reference standard. To evaluate the influence of vessel size, the total coronary vessel lumen volume relative to left ventricular mass (volume-to-mass ratio) was calculated and compared with that of patients with stable angina.

RESULTS The study evaluated 124 nonculprit vessels from 60 patients. Accuracy, sensitivity, and specificity of FFR_{CT} were 72%, 83%, and 66% versus 64% ($p = 0.033$), 93% ($p = 0.15$), and 49% ($p < 0.001$) for CTA and 72% ($p = 1.00$), 76% ($p = 0.46$), and 70% ($p = 0.54$) for invasive coronary angiography. Following STEMI, median volume-to-mass ratio was lower than in patients with stable angina, 53 versus 65 mm^3/g ($p = 0.009$). In patients with volume-to-mass ratio ≥65 mm^3/g (upper tertile) accuracy, sensitivity, and specificity of FFR_{CT} were all 83% versus 56% ($p = 0.009$), 75% ($p = 0.61$), and 44% ($p = 0.003$) in patients with <49 mm^3/g (lower tertile).

CONCLUSIONS The diagnostic performance of FFR_{CT} for staged detection of ischemia in STEMI patients with multivessel disease is moderate. STEMI patients have a smaller vessel volume than do patients with stable angina. The diagnostic performance of FFR_{CT} is influenced by the volume-to-mass ratio. This study does not support routine use of FFR_{CT} in the post-STEMI setting. (Assessment of Coronary Stenoses Using Coronary CT-Angiography and Noninvasive Fractional Flow Reserve; NCT01739075) (J Am Coll Cardiol Img 2017;10:424–33) © 2017 by the American College of Cardiology Foundation.

From the [a]Department of Cardiology, Aarhus University Hospital, Aarhus, Denmark; [b]HeartFlow, Inc., Redwood City, California; [c]Department of Bioengineering, Stanford University, Stanford, California; [d]Department of Radiology and Division of Cardiology, St. Paul's Hospital, Vancouver, British Columbia, Canada; [e]Department of Surgery, Stanford University, Stanford, California; [f]Department of Cardiology, University of Erlangen, Erlangen, Germany; and the [g]Cardiovascular Imaging Core Laboratory, Harrington Heart and Vascular Institute, Case Medical Center, Cleveland, Ohio. Drs. Taylor and Zarins are founders, employees, and shareholders of HeartFlow. Dr. Jensen has received speaker's honorarium from Bracco Imaging. Dr. Christiansen has received research grants from St. Jude Medical. Dr. Holm has received institutional research grants from St. Jude Medical, Medis Medical Imaging, and Boston Scientific. Dr. Leipsic serves as a consultant for GE Healthcare, Edwards Lifesciences, HeartFlow, Samsung, Philips, and Circle Cardiovascular Imaging. Dr. Achenbach has received institutional research grants from Siemens Healthcare and Abbott Vascular. Ms. Khem and Mr. Wilk are employees of HeartFlow. Dr. Lassen has received research grants from St. Jude Medical, Biosensors, Biotronik, Boston Scientific, Radi, Terumo, and Volcano. Dr. Nørgaard has received institutional research grants from Siemens Healthcare, Edwards Lifesciences, and HeartFlow. All other authors have reported that they have no relationships relevant to the contents of this paper to disclose.

Manuscript received February 12, 2016; revised manuscript received April 27, 2016, accepted May 4, 2016.

Primary percutaneous coronary intervention (PCI) is well established in patients with ST-segment elevation myocardial infarction (STEMI) (1,2). Approximately 50% of patients with STEMI have multivessel disease, a condition associated with increased incidence of recurrent ischemia and augmented mortality (3,4). Whether to perform revascularization of nonculprit lesions in STEMI—and when to do it—remains controversial (1,5). Current guidelines from the European Society of Cardiology/European Association for Cardio-Thoracic Surgery recommend staged revascularization of nonculprit lesions based on symptoms or evidence of ischemia (1). In the recently updated guidelines from the American College of Cardiology/American Heart Association, PCI of nonculprit vessels in STEMI may be considered, either at the time of primary PCI or as a staged procedure (2). Although fractional flow reserve (FFR) following STEMI may be affected by vessel remodeling (6,7), it has been shown that a strategy of staged complete

SEE PAGE 434

FFR-guided revascularization compared with a culprit lesion-only strategy is associated with improved clinical outcomes (8). A method of noninvasive computation of FFR from standard acquired coronary computed tomography angiography (CTA) datasets (FFR_{CT}) has been developed (9). The diagnostic performance of FFR_{CT} for identifying ischemia-causing lesions using FFR as the reference standard is high and superior to anatomical interpretation in patients with stable angina (10–12). We hypothesized that noninvasive FFR_{CT} assessment of nonculprit lesions following STEMI may be useful to guide staged revascularization. Thus, the aim of this study was to determine the diagnostic performance of FFR_{CT} for identification of ischemia-causing nonculprit lesions following STEMI using FFR as the reference standard. Furthermore, we aimed to investigate differences in variables potentially affecting the diagnostic performance of FFR_{CT} between patients with recent STEMI and patients suspected of stable angina including data from the recent NXT (HeartFlow Analysis of Coronary Blood Flow Using CT Angiography: Next Steps) trial (12).

METHODS

STUDY DESIGN. This was a prospective, single center study comprising STEMI patients with multivessel disease. The local ethics committee approved the study protocol. All patients provided written informed consent.

STUDY POPULATION. STEMI patients undergoing primary PCI with ≥1 potentially significant lesion in ≥1 nonculprit vessel determined by the interventionalist were eligible for inclusion. STEMI was defined as chest pain of <12-h duration and new ST-segment elevation ≥0.1 mV (≥0.2 mV in V_1 to V_3) involving at least 2 contiguous leads. Study exclusion criteria were hemodynamic instability, allergy to iodinated contrast, plasma creatinine ≥125 μmol/l, atrial fibrillation, contraindications to beta-receptor blocking agents, nitroglycerin or adenosine, age <18 years, body mass index >35 kg/m^2, or pregnancy.

CORONARY CTA IMAGE ACQUISITION AND ANALYSIS. Coronary CTA was performed 1 month after STEMI using a Siemens SOMATOM Definition Flash Dual Source scanner (Erlangen, Germany) (12). Image acquisition was performed in accordance with societal guidelines (13). Intravenous beta-blockers were administered if necessary, targeting a heart rate <60 beats/min, and all patients received 0.8 mg sublingual nitroglycerin. An initial 120-kV high-pitch spiral nonenhanced scan for calcium scoring was performed. Further details are provided in the Online Appendix. Scans were assessed using axial images and multiplanar reconstructions by 2 experienced cardiologists blinded to patient characteristics and other test results. In an 18-segment coronary model, vessel segments ≥2 mm were evaluated for lumen narrowing (12). Coronary stenosis >50% was considered obstructive.

COMPUTATION OF FFR_{CT}. FFR_{CT} analysis was performed in a blinded fashion using software version 1.4 (HeartFlow Inc., Redwood City, California) (12). Based on the coronary CTA images, an individual quantitative 3-dimensional anatomical model of the epicardial coronary arteries, the aortic root, and the myocardium was generated. All stents deployed at the primary PCI procedure were assumed patent. Using computational fluid dynamics principles, coronary blood flow and pressure were computed under simulated hyperemic conditions (9). Lesion-specific ischemia was defined as FFR_{CT} ≤0.80.

CALCULATION OF VOLUME-TO-MASS RATIO. The volumes of all vessels in the image-based anatomical model were assessed. Moreover, to extend the latter down to pre-capillary levels, coronary morphometric data were generated using branching laws (14). The total coronary artery lumen volume was calculated from the combined image-based and morphometric data. The volume of the myocardium extracted from

ABBREVIATIONS AND ACRONYMS

CI = confidence interval

CTA = computed tomography angiography

FFR = fractional flow reserve

FFR_{CT} = fractional flow reserve derived from computed tomography angiography datasets

ICA = invasive coronary angiography

IQR = interquartile range

PCI = percutaneous coronary intervention

STEMI = ST-segment elevation myocardial infarction

the image data was multiplied by an average value of myocardial tissue density (1.05 g/ml) to calculate the left ventricular myocardial mass (9,15). To adjust the vessel lumen volume for differences in size of the supplied myocardium, the vessel volume relative to myocardial mass (volume-to-mass ratio) was computed by dividing the total coronary artery lumen volume by the left ventricular myocardial mass.

QUANTITATIVE CORONARY ANGIOGRAPHY. Invasive coronary angiography (ICA), scheduled 1 day after coronary CTA, was performed in accordance with standard practice (12). Two projections were obtained in each major epicardial coronary artery with angles of projection optimized based on cardiac position. Stenosis severity was determined by standard quantitative coronary angiography in a blinded fashion (QAngio XA 7.3, Medis Medical Imaging Systems, Leiden, the Netherlands) (16). Stenosis severity >50% was considered obstructive.

FFR. During the staged ICA procedure, FFR interrogation was recommended in all major epicardial vessels. However, the final decision regarding FFR interrogation was at the discretion of the interventionalist. Intracoronary nitroglycerin was administered to ensure epicardial vasodilation. Hyperemia was attained by administration of adenosine (140 to 180 μg/kg/min) in a femoral or antecubital vein. A pressure-monitoring guidewire (PrimeWire Prestige PLUS, Volcano Corporation, San Diego, California) was advanced to the distal part of the vessel. Two independent blinded readers interpreted the FFR tracings. In case of discrepancy between readers, consensus was made after reinspection of the FFR tracings.

INTEGRATION OF CORONARY CTA AND FFR. The FFR_{CT} core laboratory provided a blank 3-dimensional computer model of the coronary arteries. On this model, the location(s) that corresponded to the location(s) of the distal pressure sensor was marked. The model was returned to the FFR_{CT} core laboratory, which reported the FFR_{CT} values at the respective sites.

RADIATION EXPOSURE. Cumulative radiation exposures were reported in millisievert. For coronary CTA, the formula used was: mSv = (dose length product) × 0.014, for ICA, a conversion factor of 0.18 mSv/(Gy · cm^2) was applied (17).

COMPARISONS BETWEEN PATIENTS WITH STEMI AND PATIENTS WITH STABLE ANGINA. Variables associated with coronary CTA image quality (body mass index, heart rate, and Agatston score) were compared between the present study population and the population of the NXT trial (12). Cohorts from the present study population and the NXT trial matched 1:1 with respect to age, sex, and Agatston score were identified and compared with regard to body mass index and heart rate. Based on a strikingly low vessel size despite administration of nitroglycerin in most STEMI patients observed during the study period, we hypothesized that the volume-to-mass ratio would provide insight into the diagnostic performance of FFR_{CT}. Thus, post hoc analyses of the volume-to-mass ratio between the present study and patients from the NXT trial were performed.

TWELVE MONTHS FOLLOW-UP. Data on unplanned (clinically driven) ICA and revascularization procedures and repeat myocardial infarction, respectively, were obtained from patient files and registries (18) within 12 months after the ICA 1-month study procedure.

STATISTICAL ANALYSIS. Continuous variables are presented as mean ± SD and range or medians (interquartile range [IQR]) as appropriate. Categorical variables are presented as numbers and percentages. Data were compared by paired or unpaired Student *t* test, the Wilcoxon signed rank test, or the chi-square test as appropriate. The relationship between FFR_{CT} and FFR was assessed by Pearson correlation coefficient. The reference standard for lesion-specific ischemia was FFR ≤0.80 (8,10–12). The per-vessel diagnostic performance of coronary stenosis >50% determined by coronary CTA or ICA and FFR_{CT} ≤0.80 was assessed by accuracy, sensitivity, specificity, positive predictive value, and negative predictive value. Identification of ischemia by coronary CTA, FFR_{CT}, and ICA was assessed by the area under the receiver-operating characteristics curve. Normal-based bootstrapping with 10,000 samples was used for adjustment for clustering effects in the 95% confidence intervals (CI), and for comparison of diagnostic performance estimates. The primary diagnostic performance analyses comprised all nonculprit vessels. Secondary analyses included assessment of the diagnostic performance of FFR_{CT} in relation to volume-to-mass ratio and Agatston score. Subanalyses relating per-vessel coronary CTA, ICA, and FFR_{CT} to downstream revascularization were performed. Statistical analysis was performed with Stata software version 12 (StataCorp, College Station, Texas).

RESULTS

Sixty patients recruited between February 2012 and February 2014 comprised the study population (**Figure 1**). Interrogation by FFR was performed in 168 vessels, of which 124 (74%) were of nonculprit origin.

Discrepancies in FFR interpretation between the 2 readers were solved by consensus in 3 vessels (2%) from 3 patients (5%).

Baseline characteristics are shown in **Table 1**. Details regarding the primary PCI procedure and post-procedural medication are shown in Online Table 1. No patients were readmitted to hospital or underwent unscheduled ICA between primary PCI and coronary CTA. Characteristics of study procedures are provided in Online Table 2. At the time of coronary CTA, left ventricular ejection fraction was ≥50% in 51 patients (85%). The mean interval between primary PCI and coronary CTA was 38 days, and mean interval between coronary CTA and ICA was 1 day. For patients not undergoing PCI after follow-up ICA (n = 30), mean estimated effective radiation dose was 6.2 ± 1.7 mSv for the ICA versus 2.8 ± 1.3 mSv for the coronary CTA procedure ($p < 0.001$). Per-patient and per-vessel characteristics according to the coronary CTA, FFR_{CT}, ICA, and FFR results are shown in **Table 2**. All stents were patent at follow-up ICA. Mean FFR_{CT} and FFR across nonculprit lesions were 0.79 ± 0.11 (range 0.49 to 0.96) and 0.85 ± 0.13 (range 0.32 to 1.00) ($p < 0.001$). Overall, mean heart rate during coronary CTA and Agatston score, median volume-to-mass ratio in the present cohort in comparison with the 254 patients from the NXT trial were 58 ± 8 beats/min versus 63 ± 10 beats/min ($p = 0.001$), 398 ± 431 versus 302 ± 467 ($p = 0.015$), and 53 mm^3/g (IQR: 39 to 72 mm^3/g) versus 65 mm^3/g (IQR: 45 to 94 mm^3/g) ($p = 0.009$), respectively. In the present study cohort, median volume-to-mass ratio was 53 (IQR: 39 to 79) among smokers and 54 (IQR: 34 to 61) among nonsmokers ($p = 0.51$).

DIAGNOSTIC PERFORMANCE OF CORONARY CTA, FFR_{CT}, AND ICA. Diagnostic performance estimates of FFR_{CT}, coronary CTA, and ICA are shown in **Table 3**. Compared with coronary CTA alone, FFR_{CT} improved accuracy, specificity, and positive predictive value, whereas there was no difference between FFR_{CT} and ICA estimates. Overall, FFR_{CT} did not improve the discrimination of lesion-specific ischemia when compared with anatomical assessment by coronary CTA or ICA (Online Figure 1). Agreement in detection of lesion-specific ischemia between coronary CTA, FFR_{CT}, and ICA is shown in Online Table 3. Median volume-to-mass ratio in vessels correctly or incorrectly classified by FFR_{CT} were 56 mm^3/g (IQR: 49 to 84 mm^3/g) and 49 mm^3/g (IQR: 33 to 57 mm^3/g) ($p = 0.02$), respectively. **Figure 2** displays a patient case.

SUBGROUP ANALYSES. In an analysis comprising all (including culprit) vessels (n = 168), accuracy, sensitivity, specificity, and area under the receiver-operating characteristics curve of FFR_{CT} were unaltered. The diagnostic performance of FFR_{CT} remained equivalent to that of ICA when analyses were restricted to vessels with lesions adjudicated by the interventionalist during the primary PCI procedure as potentially significant (n = 82). In vessels with or without lesions adjudicated as

FIGURE 1 Study Enrollment

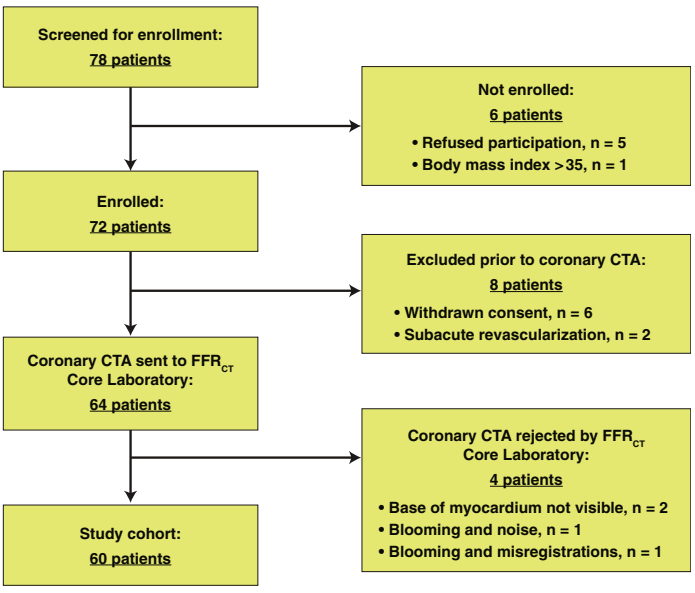

Among 72 enrolled patients, 8 (11%) were excluded prior to study procedures and 4 (6%) were excluded due to computed tomography image quality unacceptable for fractional flow reserve (FFR) derived from computed tomography angiography (CTA) datasets (FFR_{CT}) analysis. The final study cohort comprised 60 patients.

TABLE 1 Baseline Characteristics

	STEMI Study Cohort (n = 60)	NXT Trial Cohort (n = 254)
Age, yrs	61 ± 10	64 ± 10
Male	50 (83)	162 (64)*
Family history of premature atherosclerotic disease	27 (45)	79 (33)
Previous myocardial infarction	1 (2)	5 (2)
Previous PCI	1 (2)	0 (0)*
Hypertension	21 (35)	174 (69)*
Hypercholesterolemia	17 (28)	200 (79)*
Diabetes	6 (10)	58 (23)*
Current smoker	39 (65)	46 (18)*
Body mass index, kg/m^2	26 ± 4	26 ± 3
Plasma-creatinine, mg/dl	0.8 ± 0.2	0.9 ± 0.2

Values are mean ± SD or n (%). *$p < 0.05$.

NXT = HeartFlow Analysis of Coronary Blood Flow Using CT Angiography: Next Steps trial; PCI = percutaneous coronary intervention; STEMI = ST-segment elevation myocardial infarction.

TABLE 2 Patient and Vessel Characteristics by Coronary CTA, FFR$_{CT}$, Staged ICA, and FFR

Patients	
Maximum stenosis on coronary CTA >50%	57 (95)
Maximum stenosis on coronary CTA >70%	34 (57)
Intermediate-range stenosis on coronary CTA (30%-70%)	43 (72)
ICA maximum stenosis >50%	43 (72)
ICA maximum stenosis >70%	3 (5)
FFR$_{CT}$ ≤0.80	46 (77)
FFR ≤0.80	35 (58)
FFR ≤0.80 in >1 vessel	7 (12)
Agatston score*	398 ± 431 (range 0–2,082; IQR: 89–586)
Vessels	
Maximum stenosis on coronary CTA >50%	81 (65)
Maximum stenosis on coronary CTA >70%	39 (31)
Intermediate-range stenosis on coronary CTA (30%-70%)	63 (51)
ICA stenosis >50%	57 (46)
ICA stenosis >70%	3 (2)
FFR$_{CT}$ ≤0.80	63 (51)
FFR ≤0.80	42 (34)

Values are n (%) or mean ± SD (range; IQR). n = 60 patients and 124 vessels.
*Agatston score available in 57 patients.

CTA = computed tomography angiography; FFR = fractional flow reserve; FFR$_{CT}$ = fractional flow reserve derived from computed tomography angiography datasets; ICA = invasive coronary angiography; IQR = interquartile range.

significant during primary PCI, FFR was ≤0.80 in 39 of 82 (48%) and 3 of 42 (7%), respectively. In the latter 3 vessels, FFR$_{CT}$ was ≤0.80. Findings were consistent independent of the arterial distribution and number of stents. FFR$_{CT}$ was superior to coronary CTA for prediction of downstream revascularization (Online Table 4).

In a matched analysis (n = 53) comparing the present study cohort with the NXT cohort, mean body mass index was 26 ± 4 kg/m^2 versus 26 ± 3 kg/m^2 (p = 0.50) and mean heart rate was 58 ± 8 beats/min versus 62 ± 9 beats/min (p = 0.08). In the matched analysis, 2 patients (4%) from the NXT cohort versus 100% in the STEMI study cohort had a history of previous myocardial infarction. The median volume-to-mass ratio tended to be lower in the STEMI study cohort than in the matched NXT cohort, 53 mm^3/g (IQR: 37 to 79 mm^3/g) versus 61 mm^3/g (IQR: 47 to 87 mm^3/g) (p = 0.08). The diagnostic performance of FFR$_{CT}$ in the present study was highest in the volume-to-mass ratio upper tertile (Figure 3) with accuracy of 83% (95% CI: 71% to 95%), sensitivity 83% (95% CI: 60% to 100%), and specificity 83% (95% CI: 68% to 99%) in comparison with 71% (95% CI: 59% to 84%) (p = 0.12), 100% (95% CI: 74% to 100%) (p = 0.15), and 60% (95% CI: 45% to 75%) (p = 0.016) for coronary CTA and 81% (95% CI: 68% to 94%) (p = 0.75), 92% (95% CI: 75% to 100%) (p = 0.59), and 77% (95% CI: 60% to 93%) (p = 0.42) for ICA. Overall, results were consistent when following a volume-to-mass ratio binary analysis approach. In vessels with low to intermediate volume-to-mass ratio and high Agatston score, the diagnostic performance of FFR$_{CT}$ was poor (Figure 4). If the latter group of vessels was excluded from analysis, accuracy, sensitivity, and specificity of FFR$_{CT}$ in 95 vessels increased to 80% (95% CI: 72% to 88%), 90% (95% CI: 79% to 100%), and 75% (95% CI: 64% to 86%), respectively.

FOLLOW-UP. Over 12 months of follow-up, 8 patients (13%) underwent unplanned ICA with revascularization (PCI in all) performed in 6 (10%). PCI was performed in 10 lesions, of which 7 were assessed at the 1-month coronary CTA and ICA studies. In 6 and 4 lesions, stenosis was >50% by coronary CTA and ICA, respectively. In 5 and 2 lesions, FFR$_{CT}$ and FFR were ≤0.80. Median FFR$_{CT}$ and FFR were 0.76 (IQR: 0.67 to 0.81; range 0.50 to 0.88) and 0.87 (IQR: 0.69 to 0.91; range 0.68 to 0.93), respectively. Median volume-to-mass ratio in these patients was 40 mm^3/g (IQR: 28 to 56 mm^3/g; range 25 to 97 mm^3/g). No patients suffered a new myocardial infarction.

CORRELATION BETWEEN FFR$_{CT}$ AND FFR. There was a moderate direct correlation between FFR$_{CT}$ and

TABLE 3 Diagnostic Performance of Coronary CTA, FFR$_{CT}$, and ICA for Detection of FFR ≤0.80

	CTA Stenosis >50%	p Value for Comparison of CTA and FFR$_{CT}$	FFR$_{CT}$ ≤0.80	p Value for Comparison of FFR$_{CT}$ and ICA	ICA Stenosis >50%
Accuracy	64 (54-73)	0.033	72 (63-81)	1.00	72 (64-79)
Sensitivity	93 (85-100)	0.15	83 (72-95)	0.46	76 (62-90)
Specificity	49 (37-60)	<0.001	66 (54-78)	0.54	70 (59-80)
PPV	48 (36-60)	0.032	56 (42-69)	0.91	56 (43-70)
NPV	93 (85-100)	0.34	89 (81-96)	0.54	85 (77-93)

Values are proportions in % (95% confidence interval). n = 124 vessels.
NPV = negative predictive value; PPV = positive predictive value; other abbreviations as in Table 2.

FIGURE 2 Patient Case

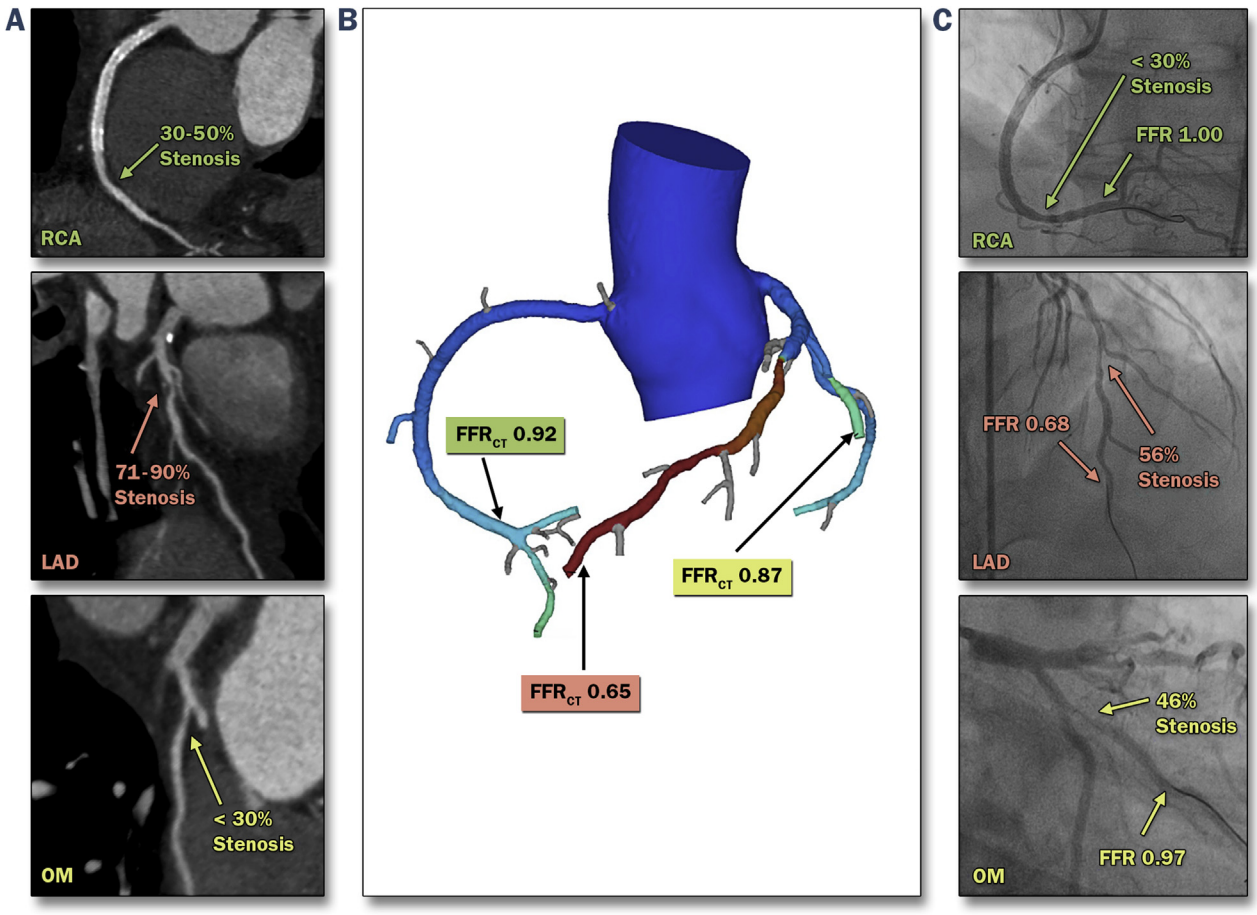

A 61-year-old man was admitted with inferior ST-segment elevation myocardial infarction. The right coronary artery (RCA) culprit lesion was treated with percutaneous coronary intervention. Nonculprit lesions were observed in the left anterior descending artery (LAD) and the first obtuse marginal branch (OM). Coronary CTA and staged invasive coronary angiography with measurement of FFR were performed after 30 and 31 days, respectively. **(A)** Coronary CTA demonstrated stenoses in the LAD, OM, and distally to the stent in RCA. **(B)** FFR_{CT} was 0.65 distal to the LAD stenosis and 0.87 in the OM. **(C)** Quantitative coronary angiography demonstrated maximal stenosis of 56% in LAD and 46% in OM. The stenosis in LAD was hemodynamically significant (FFR 0.68), whereas the stenosis in OM was not (FFR 0.97). Abbreviations as in Figure 1.

FFR with Pearson correlation coefficient 0.57 (95% CI: 0.44 to 0.68; $p < 0.001$). In the highest tertile of volume-to-mass ratio, the Pearson correlation coefficient was 0.60 (95% CI: 0.36 to 0.76; $p < 0.001$) compared with 0.43 (95% CI: 0.14 to 0.65; $p = 0.005$) in the lowest tertile. The agreement between FFR_{CT} and FFR is illustrated in Figure 5.

DISCUSSION

Three previous multicenter prospective trials including patients with suspected or known stable coronary artery disease have shown high diagnostic performance of FFR_{CT} using FFR as the reference standard (10–12). The most recent NXT trial demonstrated superior per-vessel accuracy (86%) and specificity (86%) of FFR_{CT} for detection of ischemia compared with anatomical interpretation by coronary CTA or ICA (12). In STEMI patients, a strategy of ischemia testing prior to decision making regarding revascularization of nonculprit lesions is in accordance with guidelines (1). The fact that these patients frequently are asymptomatic encourages a noninvasive diagnostic approach (5). In the present study, the diagnostic performance of FFR_{CT} for staged assessment of nonculprit lesions following STEMI was

FIGURE 3 Diagnostic Performance of FFR_{CT} According to Tertile of Volume-to-Mass Ratio

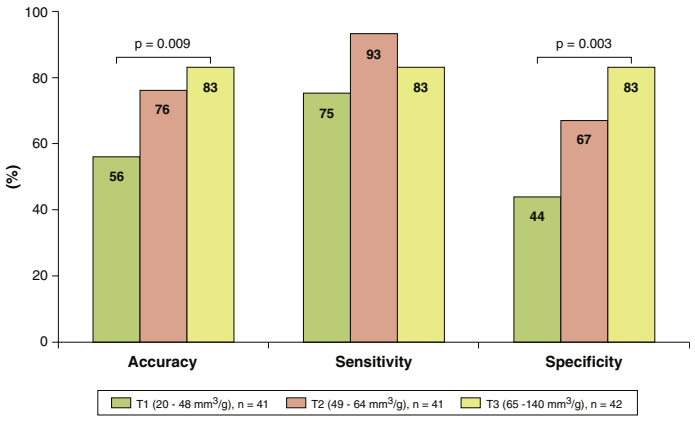

Significant p values for comparison of tertiles (T) T1 and T3 are shown; all other comparisons were statistically insignificant.

investigated for the first time. The overall diagnostic performance of FFR_{CT} for detection of ischemia-causing lesions was superior to anatomical assessment by coronary CTA and equivalent to invasive assessment by ICA. Surprisingly, the diagnostic performance of FFR_{CT} was lower than previously shown in patients with stable angina (10–12). As a potential explanation, post hoc we demonstrated that the STEMI cohort had a substantially lower volume-to-mass ratio than did patients with stable angina. Moreover, we exhibited that increasing volume-to-mass ratio in the post-STEMI setting was positively associated with the diagnostic performance of FFR_{CT}. In fact, in vessels with the highest tertile of volume-to-mass ratio (≥65 mm^3/g, comparable to the ratio in patients with stable angina from the NXT trial), the FFR_{CT} diagnostic performance was comparable to the findings in the NXT trial (accuracy 83%, sensitivity 83%, specificity 83%). In contrast, in vessels with the lowest volume-to-mass ratio (<49 mm^3/g), FFR_{CT} demonstrated poor diagnostic performance (accuracy 56%, specificity 44%). These observations as well as the clinical benefit and safety in the post-STEMI setting of a noninvasive anatomical-functional approach by coronary CTA and FFR_{CT} need further delineation in future and larger studies.

To the best of our knowledge, no previous study has assessed changes in vessel lumen volume for an extended period after STEMI. However, several factors may modulate coronary remodeling following STEMI. Low coronary blood flow causes adaptive reduction in vessel size (9). In the acute setting of STEMI, a reduction in coronary blood flow has been demonstrated in both culprit and nonculprit vessels (19). During the convalescence phase following STEMI, patients may be less physically active than stable patients. The resultant decrease in myocardial oxygen demand may reduce the coronary blood flow and/or the vasodilatory capacity. Alpha-adrenergic blockade attenuates vasoconstriction in nonculprit vessels after STEMI (20). Furthermore, a reduced microvasculatory vasodilator response has been observed up to 6 months following myocardial infarction in the perfusion beds of both culprit and nonculprit vessels (6,7). In a recent study, there was a decrease in FFR (mean 0.92 to 0.89) and an increase in coronary flow reserve (mean 2.3 to 3.1) from day 1 to 6 months after STEMI that could not be explained by changes in anatomy (7). Thus, adaptation to low flow, local neurohumoral reflexes resulting in epicardial vasoconstriction, and attenuated vasodilatory capacity are possible mechanisms for the reduced volume-to-mass ratio in the present setting. It may be speculated that the microvascular resistance has not stabilized in the 1-month time period between STEMI and CT/FFR assessment in the present study. Therefore, the overall low specificity of FFR_{CT} in this study may be explained by the assumption of a normal vasodilatory response in the computational model (9), a prerequisite that may not be valid in the post-STEMI setting. Inherently, FFR_{CT} may be more indicative of the functional significance of coronary lesions once the microvasculature has fully recovered from STEMI. Moreover, it may be speculated that inadequate vasodilation resulting in falsely elevated FFR values may contribute to the lower than expected correlation between FFR and FFR_{CT}. Our results are certainly hypothesis generating, thus future studies are needed to delineate the mechanisms responsible for the small volume-to-mass ratio and/or attenuated response to vasodilators following STEMI.

The finding in this study of declining diagnostic performance of both coronary CTA and FFR_{CT} in the event of low volume-to-mass ratio is in accord with previous findings showing that epicardial vasodilation mediated through administration of nitroglycerin results in recruitment of evaluable segments together with an increase in the diagnostic accuracy of coronary CTA and FFR_{CT} (21,22). Thus, despite the use of subvoxel techniques to overcome the limitations in CT spatial resolution and automated segmentation algorithms for calculation of FFR_{CT},

FIGURE 4 Diagnostic Performance of FFR_{CT} in Relation to Volume-to-Mass Ratio and Agatston Score

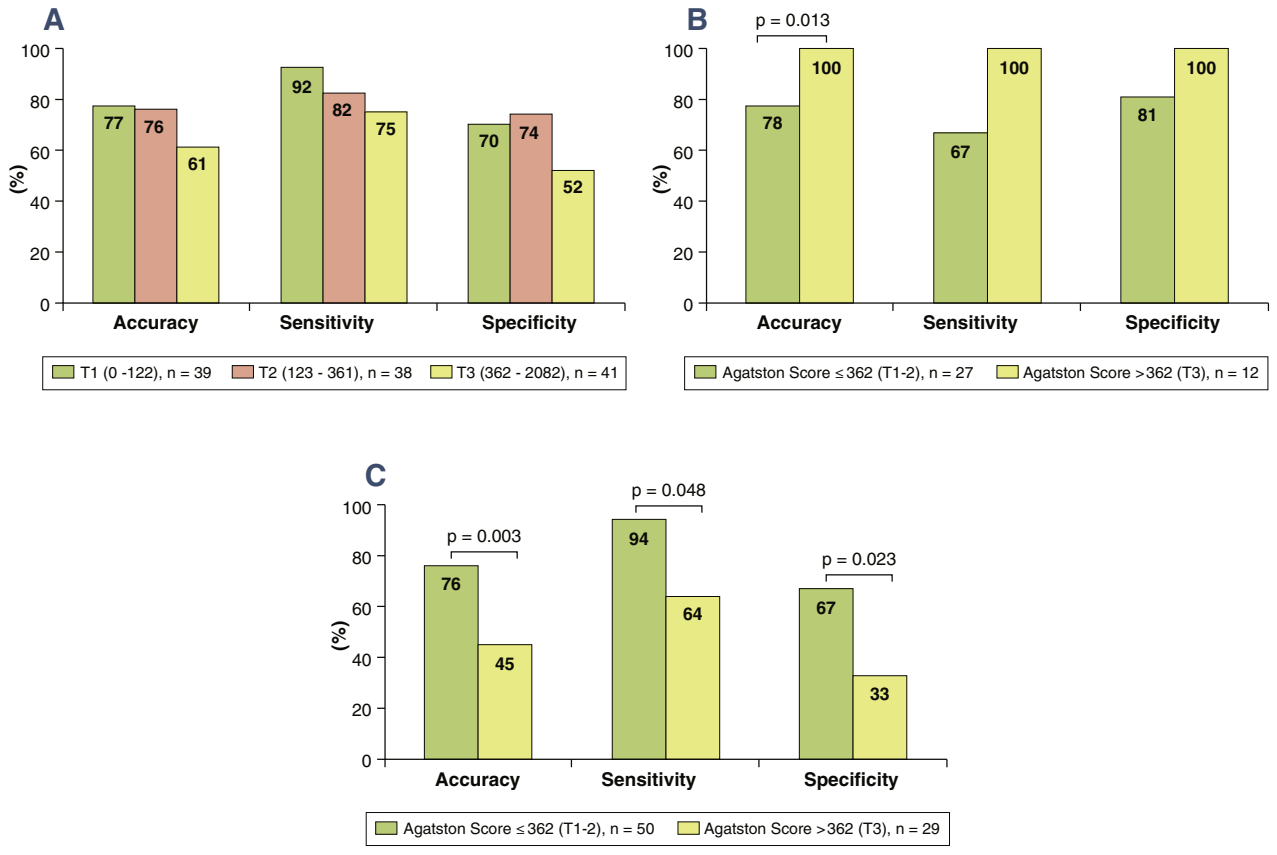

(A) Diagnostic performance of fractional flow reserve derived from computed tomography angiography datasets (FFR_{CT}) according to tertiles (T) of Agatston score. **(B)** Diagnostic performance of FFR_{CT} according to the Agatston score in vessels in the upper tertile of volume-to-mass ratio (≥65 mm^3/g). **(C)** Diagnostic performance of FFR_{CT} according to the Agatston score in the 2 lower tertiles of volume-to-mass ratio (<65 mm^3/g). Agatston score was available in 57 patients (118 vessels).

low coronary vessel size and/or attenuated vasodilatory responsiveness following STEMI seem to compromise accurate computation of FFR. It should be acknowledged that because the resistance in vessels can be approximated by Poiseuille's law as inversely related to vessel diameter to the fourth power, inadequate vessel segmentation may introduce errors in stenosis diameter and even larger errors in stenosis resistance, pressure drop, and computed FFR (9).

STUDY LIMITATIONS. This was single-center study. Because of the low number of patients, analyses were restricted to the per-vessel level. Inherently our findings may not be widely applicable. However, baseline characteristics were comparable to other studies of contemporary STEMI patients (7,8), supporting the generalizability of these findings. Study inclusion was limited by the necessity of obtaining consent within a few hours following primary PCI, as the patients, due to rules from the ethics committee, were not to be contacted regarding study inclusion after discharge from the PCI center. However, potential selection bias was caused solely by logistical reasons and was unrelated to conditions with potential effect on FFR_{CT} performance. Left ventricular function was normal or near normal in the majority of patients, thus the influence of this metric on FFR_{CT} diagnostic performance could not be assessed. As maximum troponin T levels were not recorded, the effect of biomarker levels on FFR_{CT} diagnostic performance could not be assessed. Matching for all

FIGURE 5 Agreement Between FFR and FFR$_{CT}$

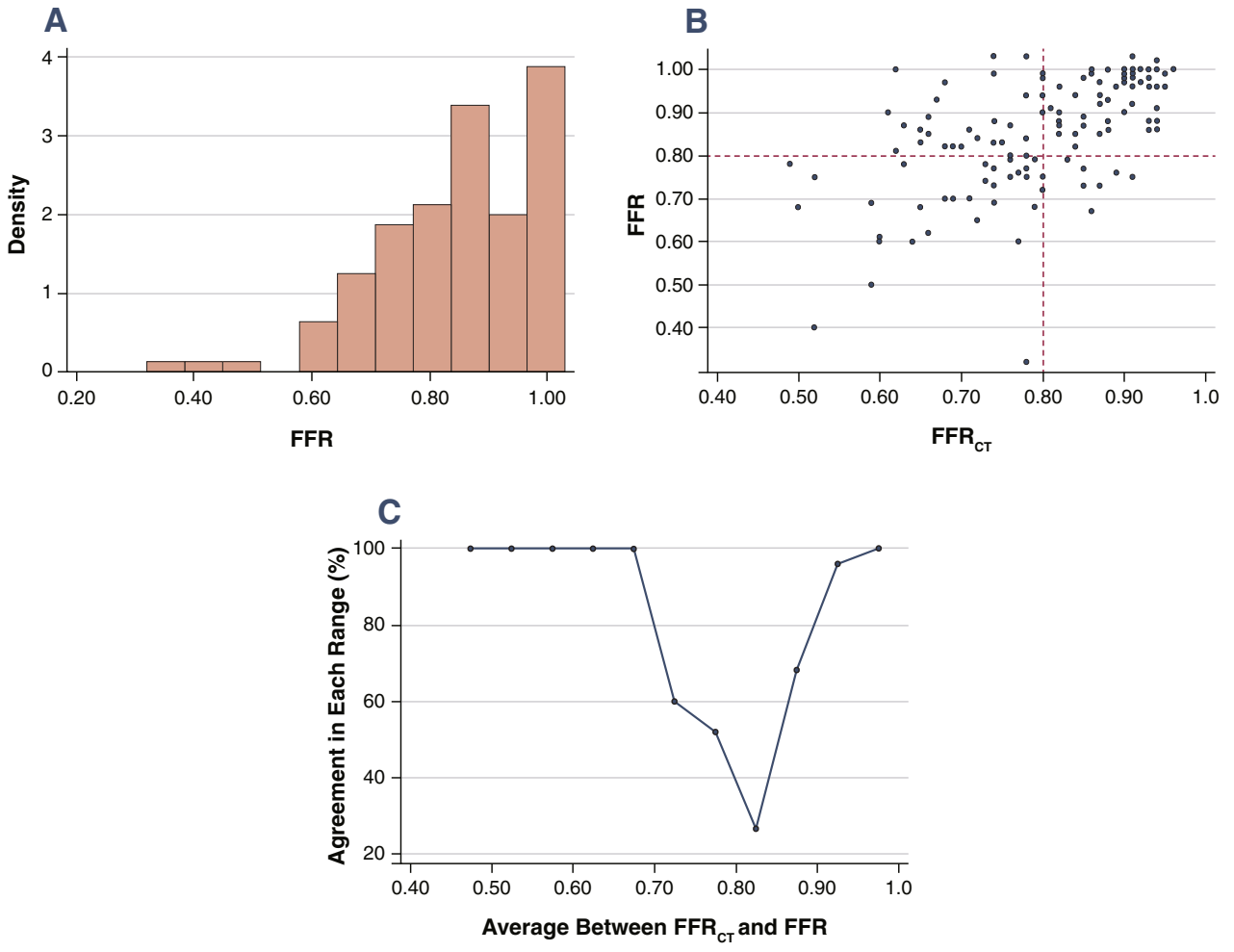

(A) Histogram of FFR values. **(B)** Scatterplot of FFR and FFR$_{CT}$. **(C)** Per-range agreement between FFR$_{CT}$ and FFR. Near the established cutoff of 0.80, the agreement reduces significantly. n = 124 vessels. Abbreviations as in Figure 1.

variables with potential significance on FFR$_{CT}$ diagnostic performance was not possible. In this study, the volume-to-mass ratio was assessed during the FFR$_{CT}$ computation process. In the future, volume-to-mass ratio may potentially be assessed locally and used as a screening tool before FFR$_{CT}$ assessment. Survival 12-month follow-up data were not available.

CONCLUSIONS

The overall diagnostic performance of FFR$_{CT}$ for staged detection of ischemia in nonculprit vessels of STEMI patients with multivessel disease is modest. Relative to patients with stable angina, STEMI patients have a reduced vessel volume. In patients with recent STEMI, the diagnostic performance of FFR$_{CT}$ is influenced by the volume-to-mass ratio. Currently there is no evidence to support FFR$_{CT}$ assessment in the post-STEMI setting. The clinical utility of FFR$_{CT}$ in patients with recent acute coronary syndromes needs further investigation.

ADDRESS FOR CORRESPONDENCE: Dr. Sara Gaur, Department of Cardiology, Aarhus University Hospital, Palle Juul-Jensens Boulevard 99, Aarhus N, Denmark 8200, Denmark. E-mail: saga@clin.au.dk.

PERSPECTIVES

COMPETENCY IN MEDICAL KNOWLEDGE: FFR_{CT} is a novel method for noninvasive computation of FFR derived from standard coronary CTA datasets using computational fluid dynamics principles. In patients with stable angina, FFR_{CT} has shown high accuracy for detection of lesion-specific ischemia compared with invasively measured FFR. In this study we demonstrated that the overall diagnostic performance of FFR_{CT} for staged detection of ischemia in nonculprit vessels of STEMI patients with multivessel disease was modest. The median coronary vessel lumen volume relative to myocardial mass (volume-to-mass) ratio was lower in the STEMI cohort than in a cohort of patients with stable angina. In patients with recent STEMI, the diagnostic performance of FFR_{CT} is influenced by the volume-to-mass ratio.

TRANSLATIONAL OUTLOOK: Currently, there is no evidence to support the use of FFR_{CT} in the post-STEMI setting. The clinical benefit and safety of noninvasive anatomical-functional assessment of nonculprit lesions by coronary CTA and FFR_{CT} need further investigation.

REFERENCES

1. Windecker S, Kolh P, Alfonso F, et al. 2014 ESC/EACTS guidelines on myocardial revascularization: the Task Force on Myocardial Revascularization of the European Society of Cardiology (ESC) and the European Association for Cardio-Thoracic Surgery (EACTS) developed with the special contribution of the European Association of Percutaneous Cardiovascular Interventions (EAPCI). Eur Heart J 2014;35:2541–619.

2. Levine GN, Bates ER, Blankenship JC, et al. 2015 ACC/AHA/SCAI focused update on primary percutaneous coronary intervention for patients with ST-elevation myocardial infarction: an update of the 2011 ACCF/AHA/SCAI guideline for percutaneous coronary intervention and the 2013 ACCF/AHA guideline for the management of ST-elevation myocardial infarction. J Am Coll Cardiol 2016;67:1235–50.

3. Park DW, Clare RM, Schulte PJ, et al. Extent, location, and clinical significance of non-infarct-related coronary artery disease among patients with ST-elevation myocardial infarction. JAMA 2014;312:2019–27.

4. Sorajja P, Gersh BJ, Cox DA, et al. Impact of multivessel disease on reperfusion success and clinical outcomes in patients undergoing primary percutaneous coronary intervention for acute myocardial infarction. Eur Heart J 2007;28:1709–16.

5. Cuisset T, Noc M. Multivessel PCI in STEMI: ready to be the recommended strategy? EuroIntervention 2014;10 Suppl T:T47–54.

6. Uren NG, Crake T, Lefroy DC, de Silva R, Davies GJ, Maseri A. Reduced coronary vasodilator function in infarcted and normal myocardium after myocardial infarction. N Engl J Med 1994;331:222–7.

7. Cuculi F, De Maria GL, Meier P, et al. Impact of microvascular obstruction on the assessment of coronary flow reserve, index of microcirculatory resistance, and fractional flow reserve after ST-segment elevation myocardial infarction. J Am Coll Cardiol 2014;64:1894–904.

8. Engstrom T, Kelbaek H, Helqvist S, et al., for the DANAMI-3—PRIMULTI Investigators. Complete revascularisation versus treatment of the culprit lesion only in patients with ST-segment elevation myocardial infarction and multivessel disease (DANAMI-3—PRIMULTI): an open-label, randomised controlled trial. Lancet 2015;386:665–71.

9. Min JK, Taylor CA, Achenbach S, et al. Noninvasive fractional flow reserve derived from coronary CT angiography: clinical data and scientific principles. J Am Coll Cardiol Img 2015;8:1209–22.

10. Koo BK, Erglis A, Doh JH, et al. Diagnosis of ischemia-causing coronary stenoses by noninvasive fractional flow reserve computed from coronary computed tomographic angiograms: results from the prospective multicenter DISCOVER-FLOW (Diagnosis of Ischemia-Causing Stenoses Obtained via Noninvasive Fractional Flow Reserve) study. J Am Coll Cardiol 2011;58:1989–97.

11. Min JK, Leipsic J, Pencina MJ, et al. Diagnostic accuracy of fractional flow reserve from anatomic CT angiography. JAMA 2012;308:1237–45.

12. Nørgaard BL, Leipsic J, Gaur S, et al., for the NXT Trial Study Group. Diagnostic performance of noninvasive fractional flow reserve derived from coronary computed tomography angiography in suspected coronary artery disease: the NXT trial (Analysis of Coronary Blood Flow Using CT Angiography: Next Steps). J Am Coll Cardiol 2014;63:1145–55.

13. Abbara S, Arbab-Zadeh A, Callister TQ, et al. SCCT guidelines for performance of coronary computed tomographic angiography: a report of the Society of Cardiovascular Computed Tomography Guidelines Committee. J Cardiovasc Comput Tomogr 2009;3:190–204.

14. Kassab GS, Rider CA, Tang NJ, Fung YC. Morphometry of pig coronary arterial trees. Am J Physiol 1993;265:H350–65.

15. Sandstede J, Lipke C, Beer M, et al. Age- and gender-specific differences in left and right ventricular cardiac function and mass determined by cine magnetic resonance imaging. Eur Radiol 2000;10:438–42.

16. Holm NR, Hojdahl H, Lassen JF, Thuesen L, Maeng M. Quantitative coronary analysis in the Nordic Bifurcation studies. Int J Cardiovasc Imaging 2011;27:175–80.

17. Einstein AJ, Moser KW, Thompson RC, Cerqueira MD, Henzlova MJ. Radiation dose to patients from cardiac diagnostic imaging. Circulation 2007;116:1290–305.

18. Nielsen LH, Norgaard BL, Tilsted HH, et al. The Western Denmark Cardiac Computed Tomography Registry: a review and validation study. Clin Epidemiol 2014;7:53–64.

19. Gibson CM, Ryan KA, Murphy SA, et al. Impaired coronary blood flow in nonculprit arteries in the setting of acute myocardial infarction: the TIMI Study Group: Thrombolysis in Myocardial Infarction. J Am Coll Cardiol 1999;34:974–82.

20. Gregorini L, Marco J, Kozakova M, et al. Alpha-adrenergic blockade improves recovery of myocardial perfusion and function after coronary stenting in patients with acute myocardial infarction. Circulation 1999;99:482–90.

21. Takx RA, Sucha D, Park J, Leiner T, Hoffmann U. Sublingual nitroglycerin administration in coronary computed tomography angiography: a systematic review. Eur Radiol 2015;25:3536–42.

22. Leipsic J, Yang TH, Thompson A, et al. CT angiography (CTA) and diagnostic performance of noninvasive fractional flow reserve: results from the Determination of Fractional Flow Reserve by Anatomic CTA (DeFACTO) study. AJR Am J Roentgenol 2014;202:989–94.

KEY WORDS coronary computed tomography angiography, fractional flow reserve, nonculprit lesion, ST-segment elevation myocardial infarction

APPENDIX For supplemental materials, please see the online version of this article.